

In-Depth DCT Coefficient Distribution Analysis for First Quantization Estimation

Sebastiano Battiato
University of Catania, Italy
battiato@dmi.unict.it

Oliver Giudice
University of Catania, Italy
giudice@dmi.unict.it

Francesco Guarnera
University of Catania, Italy
francesco.guarnera@unict.it

Giovanni Puglisi
University of Cagliari, Italy
puglisi@unica.it

Abstract— The exploitation of traces in JPEG double compressed images is of utter importance for investigations. Properly exploiting such insights, First Quantization Estimation (FQE) could be performed in order to obtain source camera model identification (CMI) and therefore reconstruct the history of a digital image. In this paper, a method able to estimate the first quantization factors for JPEG double compressed images is presented, employing a mixed statistical and Machine Learning approach. The presented solution is demonstrated to work without any a-priori assumptions about the quantization matrices. Experimental results and comparisons with the state-of-the-art show the goodness of the proposed technique.

Index Terms—FQE, Multimedia Forensics, JPEG

I. INTRODUCTION

Today, a typical life-cycle of a digital image is: (i) acquisition by means of a digital camera (often a smartphone); (ii) upload of the image to Social Network platforms or (iii) sending it through an Instant Messaging platform like Whatsapp or Telegram. The image has already gone through a double JPEG compression [1]. Thus, many information of the original image could be lost. If this image became the subject of a forensics investigation it is necessary to reconstruct its history [2] and then identifying camera model and camera source. At first, double compression must be detected ([3], [4]), subsequently camera model could be inferred employing First Quantization Estimation (FQE) and finally camera source identification could be performed by means of comparison of Photo Response Non Uniformity (PRNU) ([5], [6]).

In this paper a mixed statistical and Machine Learning approach for quantization factors estimation is presented. It employs a proper dataset of distributions for comparison, built without strong a-priori assumptions about the involved quantization matrices. Moreover, to reduce the computational complexity and the overall memory requirements, the proposed solution exploits Discrete Cosine Transform (DCT) distribution properties (i.e., AC coefficients are usually characterized by Laplacian distribution). Experimental results and comparisons demonstrated the robustness of the method.

The remainder of this paper is organized as follows: in Section II related works are discussed; Section III introduces the reader to the JPEG notation; Section IV describes the proposed novel approach with discussion on its parameters in Section V. Experimental results are reported in Section VI and finally Section VII concludes the paper.

II. RELATED WORKS

First Quantization Estimation is extremely useful for forensics investigations giving hints about the history of a digital image. Many solutions were proposed in recent years. At first research activity was involved only in estimating the first quantization factors when the information was lost due to format change (JPEG to Bitmap). Fan and De Queiroz in [7], [8] described a method to determine if an image in Bitmap format has been previously JPEG-compressed and thus they estimated the quantization matrix used. They firstly attacked this problem in an easier scenario of single compression and format change useful to understand JPEG artifacts and attract the attention of researchers until today [9].

A first robust technique for FQE was proposed by Bianchi et al. ([10], [11], [12]). They proposed a method based on the Expectation Maximization algorithm to predict the most probable quantization factors of the primary compression over a set of candidates. Other techniques based on statistical consideration of DCT histograms were proposed by Galvan et al. [13]. Their technique work at specific conditions on double compressed images exploiting the a-priori knowledge of monotonicity of the DCT coefficients. Strategies related to histogram analysis and filtering similar to Galvan et al. were introduced until these days ([14], [15]). Lately, insights used for steganography detection were exploited by Thai et al. [16]: even if they achieved good results in terms of overall accuracy, they work only at specific combinations between first and second compression factors, avoiding the estimation when quantization factors are multiples.

Given the big amount of data available today, it is easy to figure out that the problem could be evaluated by means of modern Machine Learning approaches. J. Lukáš and J. Fridrich in [17] introduced a first attempt exploiting neural networks, furtherly improved in [18] with considerations on errors similar to [13]. Convolutional Neural Networks (CNN) were recently also introduced in many papers [19], [20], [21]. CNNs have demonstrated to be incredibly powerful in finding invisible correlations on data, but they have been also very prone to what in Machine Learning is called overfitting: the situation in which the network modelled something that is not general enough to represent reality. Machine Learning techniques, and in this special case CNNs are strictly related to the dataset on which they trained. Accuracy and usability

5	5	5	5	5	5	5	5
5	5	5	5	5	5	5	5
5	5	5	5	5	5	5	5
5	5	5	5	5	5	5	5
5	5	5	5	5	5	5	5
5	5	5	5	5	5	5	5
5	5	5	5	5	5	5	5
5	5	5	5	5	5	5	5

a. M_i

3	2	2	3	5	8	10	12
2	2	3	4	5	12	12	11
2	3	3	5	8	11	14	11
3	3	4	6	10	17	16	12
4	4	7	11	14	22	21	15
5	7	11	13	16	21	23	18
10	13	16	17	21	24	24	20
14	18	19	20	22	20	21	10

b. Standard matrix $QF = 90$

Fig. 1: Example of constant matrix M_i with $i = 5$ (a), and the standard matrix corresponding to quality factor $QF = 90$ (b).

of these techniques have to be proved in "wild" conditions. Even though, state-of-the-art results are obtained recently by Niu et al. [22] where top-rated results are reported for both the aligned and not-aligned FQE scenarios.

The proposed approach, by means of a minimal set of parameters and a reference dataset, aims at surpassing the limits of both CNN-based solutions and state-of-the-art analytical ones. This could be done employing statistics on DCT coefficients in such a way to remove the need of a training phase and without falling in the limits of analytical methods, full of a-priori assumptions.

III. JPEG NOTATION

Given a raw image I , JPEG compression [23] could be defined as $I' = f_Q(I)$, where I' is the JPEG compressed image and Q is the 8×8 quantization matrix composed by the quantization factors $q_i \in \mathbb{N}$ with $i \in \{1, 2, \dots, 64\}$. Firstly $f_Q(I)$ converts I from the RGB color space to the YCbCr ones, then divides it in 8×8 non-overlapping blocks and applies the DCT. Finally, each 8×8 block is divided by Q pixel by pixel, rounded (losing information) and then encoded. In the analysis presented in this paper, only Y channel (luminance) will be considered. Let's define $I'' = f_{Q_2}(f_{Q_1}(I))$ a JPEG double compressed image, where Q_1 and Q_2 are the quantization matrices employed for the first and for the second compression respectively.

The JPEG quality factor is defined as an integer $QF \in \{1, 2, \dots, 100\}$ referred to the quantization matrix Q and describes the loss of information where $QF = 100$ and $QF = 1$ represent the minimum and maximum level of loss respectively. Various JPEG libraries could slightly change the implementation details. In this paper, we will refer to QF as the standard quantization matrix defined by JPEG for a specific quality factor. QF_i is defined as QF used for the i -th JPEG compression.

In this paper, we denote h_i the distributions of the i -th DCT coefficients in all the 8×8 blocks of I'' . Furthermore, we define as $q_{1_1}, q_{1_2}, \dots, q_{1_k}$ the k quantization factors in zig-zag order of Q_1 which are the objective of the FQE, referring to q_1 and q_2 as the general quantization factor used in the first and in the second compression respectively. Finally, for testin purposes, we refer to $q_{1_{max}}$ as the maximum value between all

the quantization factors to be predicted (in Fig. 1b $q_{1_{max}} = 5$ considering $q_{1_1}, q_{1_2}, \dots, q_{1_k}$ in zig-zag order with $k = 15$).

IV. FQE THROUGH COMPARISON

A. Retrieval distributions

The main aim of this work is the design of a solution able to properly exploit information contained in double JPEG compressed images without being affected by the typical limits of Machine Learning solutions. Specifically, in the state-of-the-art, many FQE methods have some restrictions in terms of quantization tables; for example Niu et al. [22] provide Neural Network models working only for standard matrices as Q_2 (with $QF_2 = 80/90$). Moreover, another contribution of the proposed method is the capacity to work in challenging conditions (i.e., custom matrices).

The first (and most important) part is the generation of the reference data to be exploited in comparisons for the FQE. Starting from the RAISE dataset [24], composed by 8157 high resolution images in TIFF format (uncompressed), a patch of 64×64 pixels was extracted from the center. Hence, every crop was compressed two times, employing all the combinations of constant matrix M_i (like the one shown in Figure 1a), with $i \in \{1, 2, \dots, q_{1_{max}}\}$ for the first and the second compression. Thus, generating $8157 \times 22 \times 22 = 3.947.988$ images. This dataset will be employed as a reference for comparisons, containing images double compressed by means of only those combinations of M_i which do not belong necessarily to a specific example of real quantization matrices (e.g., standard ones). This latter feature makes the overall approach generalizable on every kind of JPEG double compressed image in the aligned scenario. Moreover, it is worth noting that $q_{1_{max}} = 22$ is a good trade-off between the amount of the data to be generated (22×22 combinations) and the maximum quantization factor to be estimated.

The comparison between the JPEG double compressed image under analysis and the generated reference dataset will be done employing the DCT coefficient distributions h_i . For this reason, the first k h_i were computed and then inserted into different sub-datasets identified by the couple $\{q_1, q_2\}$.

The insights described by Lam et al. [25] have shown the usefulness of Laplacian distribution (1) over the years ([26], [27]), then we fitted the distributions h_i on them, computing μ and β to sort the sub-datasets:

$$f(x) = \frac{1}{2\beta} \exp\left(\frac{-|x - \mu|}{\beta}\right) \quad (1)$$

The final dataset is then composed as follows:

- DC_{dset} : DC distributions splitted for every possible couple $\{q_1, q_2\}$ sub-datasets, and sorted by μ ;
- AC_{dset} : AC distributions splitted for every possible couple $\{q_1, q_2\}$ sub-datasets, and sorted by β ;

B. Quantization Factor Estimation

To estimate the first k quantization factors of the first quantization matrix Q_1 , namely $\{q_{1_1}, q_{1_2}, \dots, q_{1_k}\}$, given I'' , the overall pipeline is summarized in Algorithm 1.

The estimation is done for every single $q1_i$ with $i \in \{1, 2, \dots, k\}$. Firstly, we extract the $h_i(I'')$ from I'' employing the LibJpeg C library¹, avoiding to further add truncation and rounding error. $h_i(I'')$ is then fitted on Laplacian distribution in order to extract μ and β which are then used to seek the range of candidates from the reference dataset. The usage of μ and β makes the number of candidates constant thus the computational cost to search the most similar distributions in the reference dataset is independent to its cardinality.

A JPEG file contains the quantization matrix used in the last compression; in our case Q_2 and then all the $q2_i$, allowing the selection of a specific sub-dataset. For every sub-dataset selected in this way $\{q_j, q2_i\}$ with $j \in \{1, 2, \dots, q1_{max}\}$, we extract a range of elements $D_{j, q2_i}(\mu, \beta)$ with the most similar values of μ for DC_{dset} and β for AC_{dset} and then we compare $h_i(I'')$ with those elements using χ^2 distance:

$$\chi^2(x, y) = \sum_{i=1}^m (x_i - y_i)^2 / (x_i + y_i) \quad (2)$$

where x and y represent the distributions to be compared.

For every sub-dataset $D_{j, q2_i}$, we select the lowest distance $d_{i, j}$ obtaining $q1_{max}$ distances. The minimum distance $d_{i, j}$, $j \in \{1, 2, \dots, q1_{max}\}$ indicates the corresponding sub-dataset and then the predicted $q1$ for the current i .

C. Regularization

The $d_{i, j}$ distances obtained as described in previous Section, show that a strong minimum is not always present at varying of j . Sometimes, the information contained in $h_i(I'')$ does not clearly allow the discrimination among the possible $q1_i$ candidates. To overcome this, data coming from neighbors DCT coefficients can be exploited. Specifically, starting from the empirical hypothesis that a generic $q1_i$ value is usually close to $q1_{i-1}$ and $q1_{i+1}$, instead of estimating each coefficient independently, three consecutive elements in zig-zag order are considered. For example, if $k = 15$, 13 triplets ($q1_{i-1}, q1_i, q1_{i+1}$, $i = 2, \dots, 14$) can be identified. To estimate a single triplet $q1_{i-1}, q1_i, q1_{i+1}$, a score is associated to each possible $q1$ combination. Thus, considering $q1_{max} = 22$ as the maximum $q1$ value, $22 \times 22 \times 22$ $q1$ combinations are taken into account. A proper score S is then obtained by a weighted average between a data term (C_{data}) and a regularization term (C_{reg}) as follows:

$$S = wC_{data} + (1 - w)C_{reg} \quad (3)$$

where $w \in [0, 1]$, C_{data} is the normalized sum of the three $d_{i, j}$, and C_{reg} is the regularization term that tries to minimize the difference among the considered triplet. Further details about C_{reg} setting will be provided in Section V-B.

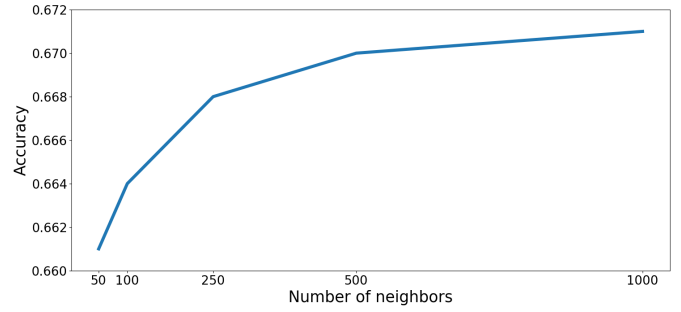


Fig. 2: Accuracy of the proposed approach w.r.t. the number of neighbors considered for comparison.

Algorithm 1 The Proposed FQE Technique

Input: double compressed image I''

Output: $\{q1_1, q1_2, \dots, q1_k\}$

Initialization: $k, q1_{max}$

```

1: for  $i = 1$  to  $k$  do
2:   if ( $i = 1$ ) then
3:      $D : DC_{dset}$ 
4:   else
5:      $D : AC_{dset}$ 
6:   end if
7:    $h_i$  : distribution of  $i$ -th DCT coefficient
8:    $\mu, \beta$  :  $\mu, \beta$  fitted on Laplacian  $h_i$ 
9:    $q2_i$  : quantization factor of  $Q_2$  for  $i$ -th DCT
10:  for  $j = 1$  to  $q1_{max}$  do
11:     $D_{j, q2_i}$  : sub-dataset ( $q1, q2$ ) with  $q1 = j, q2 = q2_i$ 
12:     $D_{j, q2_i}(\mu, \beta)$  : sub-range with most similar  $\mu, \beta$ 
13:     $d_{i, j}$  : lower  $\chi^2$  distance between  $h_i$  and  $D_{j, q2_i}$ 
14:  end for
15:   $q_i$  :  $argmin\{d_{i, j}\}, j \in \{1, 2, \dots, q1_{max}\}$ 
16: end for
17: regularize( $\{q1_1, q1_2, \dots, q1_k\}$ )
18: return  $\{q1_1, q1_2, \dots, q1_k\}$ 

```

V. PARAMETERS SETTING

The various parameters introduced in the Section IV, were set by means of a validation dataset D_V composed by 8157 images 64×64 pixels, cropped at random position from RAISE [24] original images.

A. Clustering

Fixed $q2$, the comparison dataset is composed by $q1_{max}$ different sub-datasets. In order to limit the overall computational complexity, a smart comparison strategy considering only a limited number of h_i exploiting μ and β values has been employed. We tested the method with D_V using a sub-range of 50, 100, 250, 500 and 1000 elements for each sub-dataset (see Fig. 2). It is worth noting that the value considered in the proposed solution (1000), represents a viable trade-off between accuracy and computational cost with respect to the full search solution.

¹<https://github.com/LuaDist/libjpeg>

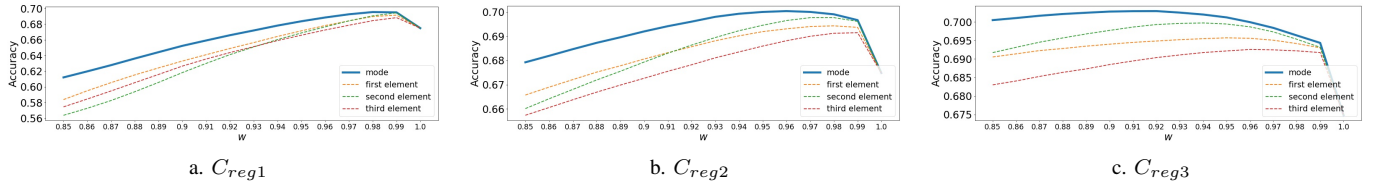


Fig. 3: a, b and c describe the accuracies obtained for different values of the regularization parameter w employing the three equations (4), (5), (6) respectively. Every plot shows the accuracies obtained considering the first, the second and the third element of the triplet of the analyzed quantization factors and the related arithmetical mode.

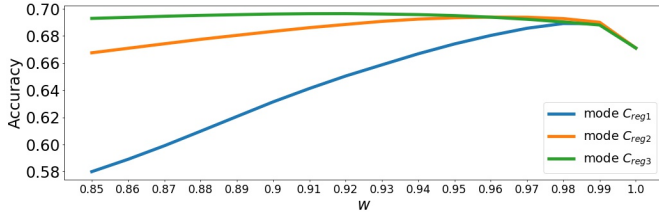


Fig. 4: Comparison between the modes of Fig. 3a, 3b, 3c

B. Regularization

In order to cope with the lack of information contained in some $h_i(I'')$, a regularization step was carried out. Triplets of the nearest $q1_i$ were estimated simultaneously, and several C_{reg} functions have been investigated:

$$C_{reg1} = \frac{(c_i - c_{i-1}) + (c_i - c_{i+1})}{2} \quad (4)$$

$$C_{reg2} = \frac{(c_i - c_{i-1}) + (c_i - c_{i+1})}{2\sqrt{c_i}} \quad (5)$$

$$C_{reg3} = \frac{(c_i - c_{i-1}) + (c_i - c_{i+1})}{2c_i} \quad (6)$$

where c_{i-1} , c_i , c_{i+1} are $q1$ candidates related to three consecutive quantization factors in zig-zag order. This regularization step provides multiple estimations for each single $q1_i$. For example the estimations of $q1_3$ can be found on 3 different triplets: $(q1_1, q1_2, q1_3)$, $(q1_2, q1_3, q1_4)$ and $(q1_3, q1_4, q1_5)$. The 3 strategies could then be tested. Figures 3a, 3b and 3c show the accuracies employing the corresponding C_{reg} , at varying of weights (see (3)) and $q1_i$ selection strategies. As suggested in Fig. 4 which shows the modes of eq. (4), (5), (6), we chose the use of eq. (6) with $w = 0.92$.

VI. EXPERIMENTAL RESULTS

The difficulty of the first quantization factor estimation task is proportional to the relative position in the quantization matrix, as reported in literature. For this reason and for the sake of comparison with the state-of-the-art, we set $k = 15$, although our method has not this specific limitation on k .

QF_1	$QF_2 = 90$					$QF_2 = 80$						
	Our	Our Reg.	[10]	[13]	[14]	[22]	Our	Our Reg.	[10]	[13]	[14]	[22]
55	0.76	0.77	0.53	0.52	0.45	0.00	0.55	0.58	0.36	0.37	0.37	0.24
60	0.82	0.82	0.53	0.56	0.47	0.64	0.55	0.60	0.27	0.37	0.38	0.50
65	0.79	0.81	0.54	0.57	0.49	0.54	0.68	0.65	0.19	0.41	0.43	0.31
70	0.85	0.85	0.43	0.57	0.51	0.66	0.67	0.75	0.19	0.50	0.49	0.50
75	0.83	0.85	0.41	0.63	0.53	0.77	0.48	0.56	0.07	0.56	0.45	0.15
80	0.81	0.83	0.29	0.61	0.45	0.81	0.12	0.11	0.00	0.00	0.00	0.00
85	0.78	0.85	0.14	0.74	0.36	0.81	0.28	0.34	0.19	0.00	0.00	0.00
90	0.30	0.24	0.00	0.00	0.00	0.02	0.16	0.19	0.06	0.00	0.00	0.48
95	0.44	0.52	0.11	0.00	0.00	0.78	0.27	0.30	0.00	0.00	0.00	0.95
98	0.49	0.57	0.00	0.00	0.00	0.76	0.42	0.42	0.01	0.00	0.00	0.21
MEAN	0.69	0.71	0.30	0.42	0.33	0.58	0.42	0.45	0.13	0.22	0.21	0.28

TABLE I: Accuracies obtained by the proposed approach compared to Bianchi et al. ([10]), Galvan et al. ([13]), Dalmia et al. ([14]) and Niu et al. ([22]) with different combinations of QF_1/QF_2 , considering standard quantization tables.

PS	$QF_2 = 90$					$QF_2 = 80$				
	Our	Our Reg.	[10]	[13]	[22]	Our	Our Reg.	[10]	[13]	[22]
5	0.80	0.78	0.56	0.58	0.05	0.65	0.68	0.26	0.46	0.07
6	0.82	0.82	0.46	0.60	0.07	0.42	0.54	0.05	0.41	0.02
7	0.83	0.83	0.41	0.58	0.07	0.62	0.68	0.15	0.48	0.08
8	0.81	0.81	0.25	0.65	0.10	0.19	0.22	0.03	0.03	0.01
9	0.55	0.61	0.02	0.47	0.02	0.26	0.28	0.19	0.00	0.07
10	0.42	0.50	0.19	0.00	0.25	0.15	0.20	0.00	0.00	0.40
11	0.45	0.52	0.04	0.00	0.69	0.37	0.38	0.01	0.00	0.24
12	0.49	0.57	0.04	0.00	0.75	0.42	0.42	0.01	0.00	0.21
MEAN	0.64	0.68	0.25	0.36	0.25	0.39	0.42	0.09	0.18	0.14

TABLE II: Accuracies obtained by the proposed approach compared to Bianchi et al. ([10]), Galvan et al. ([13]) and Niu et al. ([22]) employing custom tables for first compression. The column PS refers to custom tables used by Photoshop.

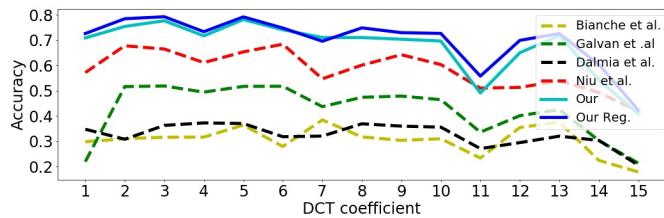
A. Comparison tests

The first set of tests has been performed to compare the proposed solution with state-of-the-art approaches based on statistical analysis (Bianchi et al. [10], Galvan et al. [13], Dalmia et al. [14]) and Machine Learning (Niu et al. [22]), employing the implementations provided by the authors.

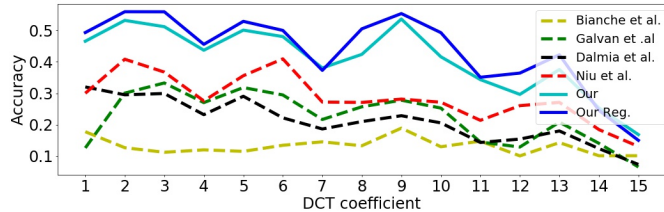
For the sake of comparison, we created 4 datasets: starting from RAISE [24], we cropped a random 64×64 patch from every image and compressed it two times as follows:

- 1) $QF_1 : \{55, 60, 65, 70, 75, 80, 85, 90, 95, 98\}$, $QF_2 : 90$
- 2) $QF_1 : \{55, 60, 65, 70, 75, 80, 85, 90, 95, 98\}$, $QF_2 : 80$
- 3) $Q_1 : \{5, 6, 7, 8, 9, 10, 11, 12\}$, $QF_2 : 90$
- 4) $Q_1 : \{5, 6, 7, 8, 9, 10, 11, 12\}$, $QF_2 : 80$

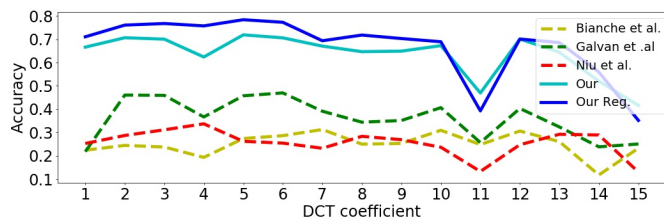
where $Q_1 : \{5, 6, 7, 8, 9, 10, 11, 12\}$ related to 3) and 4) are referred to the quantization matrices of Photoshop (CC version 20.0.4). Every method was tested with all the aforementioned



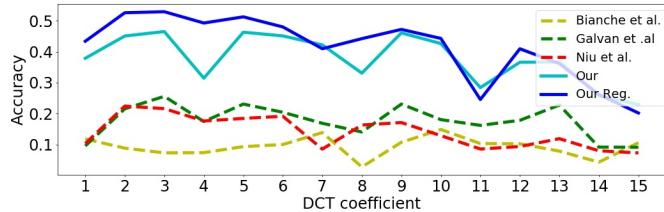
a. $QF_1 : \{55, 60, 65, 70, 75, 80, 85, 90, 95, 98\}$, $QF_2 : 90$



b. $QF_1 : \{55, 60, 65, 70, 75, 80, 85, 90, 95, 98\}$, $QF_2 : 80$



c. $Q_1 : \{5, 6, 7, 8, 9, 10, 11, 12\}$, $QF_2 : 90$



d. $Q_1 : \{5, 6, 7, 8, 9, 10, 11, 12\}$, $QF_2 : 80$

Fig. 5: Accuracies of the same methods described in Table I and II at varying of the quantization factors $q1_i$ to be predicted. The values are averaged over all the QF_1/Q_1 .

datasets with the exception of Dalmia et al. [14] which, in their implementation, make assumptions about standard tables in first compression and then was excluded in the test with Photoshop’s custom tables. Results, reported in Table I and II and in Fig. 5, clearly highlight how our method outperforms the state-of-the-art in almost all scenarios, with and without the regularization step (values close to 0 are due to the assumptions of some methods, e.g. $QF_1 < QF_2$). It is worth noting that, although the scenario employing standard matrices is the one considered by Niu et al. [22] to train their CNN, the proposed solution outperforms it with an average of **0.71** vs. **0.58** for $QF_2 = 90$ and **0.45** vs. **0.28** for $QF_2 = 80$. Differently than other Machine Learning based approaches, the proposed method, working properly also in the scenario involving Photoshop’s custom tables, demonstrates to be not

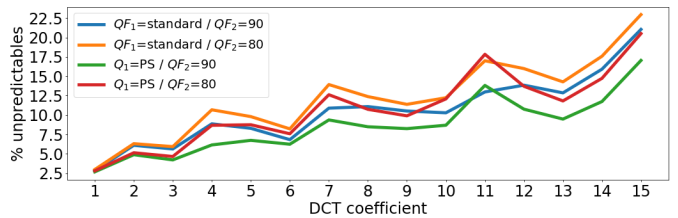


Fig. 6: Percentages of unpredictable images for the 4 described datasets at varying of DCT coefficients.

dependent to a specific class of quantization matrices.

B. Discussion on unpredictable factors

A patch extracted from an high resolution image could be too homogeneous, hence all the values of the DCT coefficients could be in the same bin of the corresponding histograms, due to the lack of variation. A patch 64×64 extracted from a RAISE image represents about the 0,033% of the information contained in the original one and then the possibility to have this homogeneous scenario is not negligible. We selected this scenario (i.e., small patches from an high resolution dataset) to test the proposed solution in a challenging condition, but we had to exclude the aforementioned histograms because they do not allow to predict the quantization factors (the available information is not enough to select a specific $q1$). In particular, given i , we exclude the distributions h_i where all the values are in the same bin of the histogram (e.g., all the i -th DCT coefficients extracted from the 8×8 blocks are equal). The percentage of $q1_i$ excluded for each dataset is shown in Figure 6 at varying of DCT coefficients.

C. Generalizing Property

Park et al. [29] proposed a collection of 1170 different quantization tables employed on real scenarios (1070 custom). In this Section, a new set of experiments will be presented in order to demonstrate the generalizing property of the proposed approach employing the same reference dataset built in Section IV-A.

From the collection of Park et al., 873 quantization tables show in the first 15 quantization factors, a value of $q1_i \leq q1_{max}$ and then they can be employed for testing. They were sorted by the average of the first 15 quantization factors and then equally divided into three sets of 291 elements (*low*, *mid*, *high*). These sets of tables are employed to create 9 combinations of double compressions (see latter 9 columns of Table III). Three new datasets for generalizing tests are then built: patches of size $w \times w$ from RAW images were extracted and then compressed two times with all the 9 aforementioned combinations. For each combination of double compression, the quantization tables (Q_1 and Q_2) are selected randomly from the 291 available in the corresponding set.

The results obtained on these three datasets are reported in Table III. They clearly show that our method maintains good accuracies on all the tested challenging scenarios and

Method	Dataset	Cropped Patch	Low/Low	Low/Mid	Low/High	Mid/Low	Mid/Mid	Mid/High	High/Low	High/Mid	High/High	Mean
Our	RAISE [24]	64 × 64	0.25	0.47	0.79	0.17	0.32	0.82	0.27	0.31	0.70	0.46
Our Reg.			0.30	0.53	0.81	0.22	0.37	0.84	0.25	0.33	0.75	0.49
Our	UCID [28]	64 × 64	0.33	0.63	0.93	0.20	0.39	0.90	0.15	0.21	0.66	0.49
Our Reg.			0.36	0.65	0.96	0.23	0.42	0.91	0.13	0.23	0.73	0.51
Our	UCID [28]	128 × 128	0.36	0.69	0.95	0.21	0.42	0.92	0.16	0.24	0.71	0.52
Our Reg.			0.37	0.71	0.95	0.24	0.43	0.92	0.24	0.33	0.74	0.55

TABLE III: Accuracies obtained by the proposed approach for generalizing property demonstration (Our Reg. for the regularized version).

demonstrates to achieve same results even when different datasets are employed for tests.

VII. CONCLUSION

In this paper, a new technique able to estimate the first quantization factors for JPEG double compressed images was presented, employing a mixed statistical and Machine Learning approach. One of the main contributions was the way we employed the big amount of data to avoid overfitting: constant matrices M_i permitted to uncouple $\{q_1, q_2\}$ and the use of μ and β made computational times acceptable. The presented solution was demonstrated to work for both custom and standard tables thus being generalizable enough to be employed in real-case scenarios. Experimental tests showed the goodness of the technique overcoming state-of-the-art results. Finally, the use of 1-nn to learn the distribution underlines rooms for improvement of the proposed method.

REFERENCES

- [1] O. Giudice, A. Paratore, M. Moltisanti, and S. Battiato, *A Classification Engine for Image Ballistics of Social Data*. Springer International Publishing, 2017, pp. 625–636 (LNCS, volume 10485).
- [2] H. Farid, “Digital image ballistics from JPEG quantization: A followup study,” *Department of Computer Science, Dartmouth College, Tech. Rep. TR2008-638*, 2008.
- [3] O. Giudice, F. Guarnera, A. Paratore, and S. Battiato, “1-D DCT domain analysis for JPEG double compression detection,” in *Proc. of International Conference on Image Analysis and Processing*. Springer, 2019, pp. 716–726 (LNCS, volume 11752).
- [4] E. Kee, M. K. Johnson, and H. Farid, “Digital image authentication from JPEG headers,” *IEEE Trans. on Information Forensics and Security*, vol. 6, no. 3, pp. 1066–1075, 2011.
- [5] A. Piva, “An overview on image forensics,” *ISRN Signal Processing*, vol. 2013, p. 22, 2013.
- [6] M. C. Stamm, M. Wu, and K. J. R. Liu, “Information forensics: An overview of the first decade,” *IEEE Access*, vol. 1, pp. 167–200, 2013.
- [7] Z. Fan and R. L. De Queiroz, “Maximum likelihood estimation of JPEG quantization table in the identification of bitmap compression history,” in *Proc. of the International Conference on Image Processing*. 1, 2000, pp. 948–951.
- [8] Z. Fan and R. De Queiroz, “Identification of bitmap compression history: JPEG detection and quantizer estimation,” *IEEE Trans. on Image Processing*, vol. 12, no. 2, pp. 230–235, 2003.
- [9] J. Yang, Y. Zhang, G. Zhu, and S. Kwong, “A clustering-based framework for improving the performance of JPEG quantization step estimation,” *IEEE Trans. on Circuits and Systems for Video Technology*, 2020.
- [10] T. Bianchi and A. Piva, “Image forgery localization via block-grained analysis of JPEG artifacts,” *Proc. of IEEE Trans. on Information Forensics and Security*, vol. 7, no. 3, p. 1003, 2012.
- [11] T. Bianchi, A. De Rosa, and A. Piva, “Improved DCT coefficient analysis for forgery localization in JPEG images,” in *Conference on Acoustics Speech and Signal Processing*, I. International, Ed. 2444, 2447: ICASSP, 2011.
- [12] A. Piva and T. Bianchi, “Detection of non-aligned double JPEG compression with estimation of primary compression parameters,” in *Proc. of 18th IEEE International Conference on Image Processing (ICIP)*, 2011. IEEE, 2011, pp. 1929–1932.
- [13] F. Galvan, G. Puglisi, A. R. Bruna, and S. Battiato, “First quantization matrix estimation from double compressed JPEG images,” *IEEE Trans. on Information Forensics and Security*, vol. 9, no. 8, pp. 1299–1310, 2014.
- [14] N. Dalmia and M. Okade, “First quantization matrix estimation for double compressed JPEG images utilizing novel dct histogram selection strategy,” in *Proc. of the Tenth Indian Conference on Computer Vision, Graphics and Image Processing*, 2016, pp. 1–8.
- [15] H. Yao, H. Wei, T. Qiao, and C. Qin, “JPEG quantization step estimation with coefficient histogram and spectrum analyses,” *Journal of Visual Communication and Image Representation*, p. 102795, 2020.
- [16] T. H. Thai and R. Cograne, “Estimation of primary quantization steps in double-compressed jpeg images using a statistical model of discrete cosine transform,” *IEEE Access*, vol. 7, pp. 76203–76216, 2019.
- [17] J. Lukáš and J. Fridrich, “Estimation of primary quantization matrix in double compressed JPEG images,” in *Proc. of the Digital Forensic Research Workshop*, 2003, pp. 5–8.
- [18] G. Varghese and A. Kumar, “Detection of double JPEG compression on color image using neural network classifier,” *International Journal*, vol. 3, pp. 175–181.
- [19] M. Barni, L. Bondi, N. Bonettini, P. Bestagini, A. Costanzo, M. Maggini, B. Tondi, and S. Tubaro, “Aligned and non-aligned double JPEG detection using convolutional neural networks,” *Journal of Visual Communication and Image Representation*, vol. 49, no. Supplement C, pp. 153 – 163, 2017.
- [20] T. Uricchio, L. Ballan, R. Caldelli, and I. Amerini, “Localization of JPEG double compression through multi-domain convolutional neural networks,” in *Proc. of the IEEE Conference on Computer Vision and Pattern Recognition Workshops*, 2017, pp. 53–59.
- [21] Q. Wang and R. Zhang, “Double JPEG compression forensics based on a convolutional neural network,” *EURASIP Journal on Information Security*, vol. 2016, no. 1, p. 23, 2016.
- [22] Y. Niu, B. Tondi, Y. Zhao, and M. Barni, “Primary quantization matrix estimation of double compressed JPEG images via CNN,” *IEEE Signal Processing Letters*, vol. 27, pp. 191–195, 2020.
- [23] G. K. Wallace, “The JPEG still picture compression standard,” *Communications of the ACM*, vol. 34, no. 4, pp. 30–44, 1991.
- [24] H. Dang-Nguyen, C. Pasquini, V. Conotter, and G. Boato, “Raise: a raw images dataset for digital image forensics,” in *Proc. of the 6th ACM Multimedia Systems Conference*, 2015, pp. 219–224.
- [25] E. Y. Lam and J. W. Goodman, “A mathematical analysis of the DCT coefficient distributions for images,” *IEEE Trans. on Image Processing*, vol. 9, no. 10, pp. 1661–1666, 2000.
- [26] D. Ravi, G. Farinella, V. Tomaselli, M. Guarnera, and S. Battiato, “Representing scenes for real-time context classification on mobile devices,” *Pattern Recognition*, vol. 48, p. 4, 2015.
- [27] X. Hou, J. Harel, and C. Koch, “Image signature: Highlighting sparse salient regions,” *IEEE transactions on pattern analysis and machine intelligence*, vol. 34, no. 1, pp. 194–201, 2011.
- [28] G. Schaefer and M. Stich, “UCID: An uncompressed color image database,” in *Storage and Retrieval Methods and Applications for Multimedia 2004*, vol. 5307. International Society for Optics and Photonics, 2003, pp. 472–480.
- [29] J. Park, D. Cho, W. Ahn, and H. Lee, “Double JPEG detection in mixed JPEG quality factors using deep convolutional neural network,” in *The European Conference on Computer Vision (ECCV)*, September 2018.